Mantle flow beneath Arabia offset from the opening Red Sea

Sung-Joon Chang[1], Miguel Merino[1], Suzan Van der Lee[1], Seth Stein[1] & Carol A. Stein[2]

[1]Department of Earth and Planetary Sciences
Northwestern University, Evanston, IL 60208, USA

[2]Department of Earth and Environmental Sciences, University of Illinois at Chicago, 845 W. Taylor Street Chicago, IL 60607-7059, USA

Supplementary Material

Method

The new seismic tomographic image of velocity structure used here is part of one of a much larger area from the marginal region of the former Tethys Ocean, which includes the Arabian Plate and the Red Sea, derived by joint inversion of seismic wave travel times and waveforms [Chang et al., 2010]. The data consist of global and regional data sets of arrival times, body wave forms, regional multimode *S* and surface wave trains, surface wave group velocities, and constraints on Moho depth from active source seismic studies, gravity surveys, global geological and geophysical interpretations, and receiver functions.

Of the regional wave trains fit in the joint inversion using the partitioned waveform inversion technique [Nolet, 1990; van der Lee and Nolet, 1997] about two and a half thousand have wave paths traverse the current study region of Arabia and the Red Sea. The data coverage is illustrated by great-circle wave paths shown by the locations of events and stations in Figure S1a. The waveform frequency content is generally somewhere between 0.006 and 0.1 Hz.

Of the Rayleigh-wave group-velocity data used [Chang et al., 2010; Pasyanos and Nyblade, 2007], with periods ranging from 7 to 100 s, nearly four thousand paths traverse the current study region. Great-circle wave paths for the 45-s period group-velocity data are shown in Figure S1b.

Of the high-resolution relative arrival times of teleseismic *S* & *SKS* waves used, about four thousand were derived by multi-channel cross correlation [vanDecar and Crosson, 1990] for receivers in Ethiopia [Beniot et al., 2006], Arabia [Park et al., 2007], and the Mediterranean region [Schmid et al., 2004]. Almost thirteen thousand additional, absolute *S* phase arrival times from the reprocessed ISC database [Engdahl et al., 1998] came from the current study region. Locations of stations and events for each type of arrival time data are depicted in Figure S1c.

Lastly, the study region here included over three hundred of the independent Moho depth estimates used in the joint inversion. These Moho depth constraints are shown in Figure S1d.

S.2. Resolution tests

Because we focus here on velocity structure below the Red Sea and Arabia, we investigated the resolving power of the joint inversion for this region with a number of different test structures using several resolution tests.

First, we tested a model with a low-velocity channel along the Red Sea and one trending northward beneath Arabia, as shown in the top-left panel of Figure S2. The resulting synthetic data were generated by multiplying the sensitivity kernels used in the inversion with the parameters of this test model. We contaminated these synthetic data with Gaussian random noise with a standard deviation proportional to the estimated uncertainty of the actual data to investigate the resolving power of the joint inversion in realistic cases. We estimate the uncertainty of the Moho constraints as 2 km for receiver function results, 4 km for active source seismic studies, and 6 km for gravity data according to data quality. Uncertainties for other data sets are given in Chang et al. [2010]. Depth slices of the inversion results at 50, 100, 150 km are shown in Figure S2. Although the anomalies are recovered with weaker amplitude than in the model, as is typical in seismic tomography, the two anomalies are distinctly resolved with similar amplitude down to at least 100 km. At 150 km depth, although the low-velocity anomaly beneath the Red Sea is recovered weakly, we can still discern both anomalies **in their correct locations, without overlap. Hence the offset of the anomaly from the Red Sea is resolved.** Moreover, the anomaly is recovered with relatively homogenous amplitude along the Red Sea, which excludes the possibility that the absence of a low-velocity anomaly beneath the northern Red Sea may be caused by poor data coverage.

We also performed a resolution test for a model including a broad low-velocity anomaly covering the Red Sea and the western half of Arabia, as shown in Figure S3. This test explored the possibility that limitations of resolving power in the joint inversion might yield an apparent narrow linear anomaly beneath Arabia. The inversion results show that the broad anomaly is well recovered without generating an artificial linear anomaly.

The first test also explored the depth resolution, as shown in cross sections along the Red Sea and the Gulf of Aden [Figure S4]. The model has low-velocity anomalies along the Red Sea, the Gulf of Aden, and beneath Arabia extending to different depths. The inversion results show that these anomalies are distinctly recovered, albeit with weaker amplitude and some smearing, as is typical in seismic tomography.

Based on these tests, we are confident that the low-velocity region beneath Arabia is a relatively narrow channel rather than a broad regional anomaly, and that this channel occurs below Arabia, not beneath the northern Red Sea.

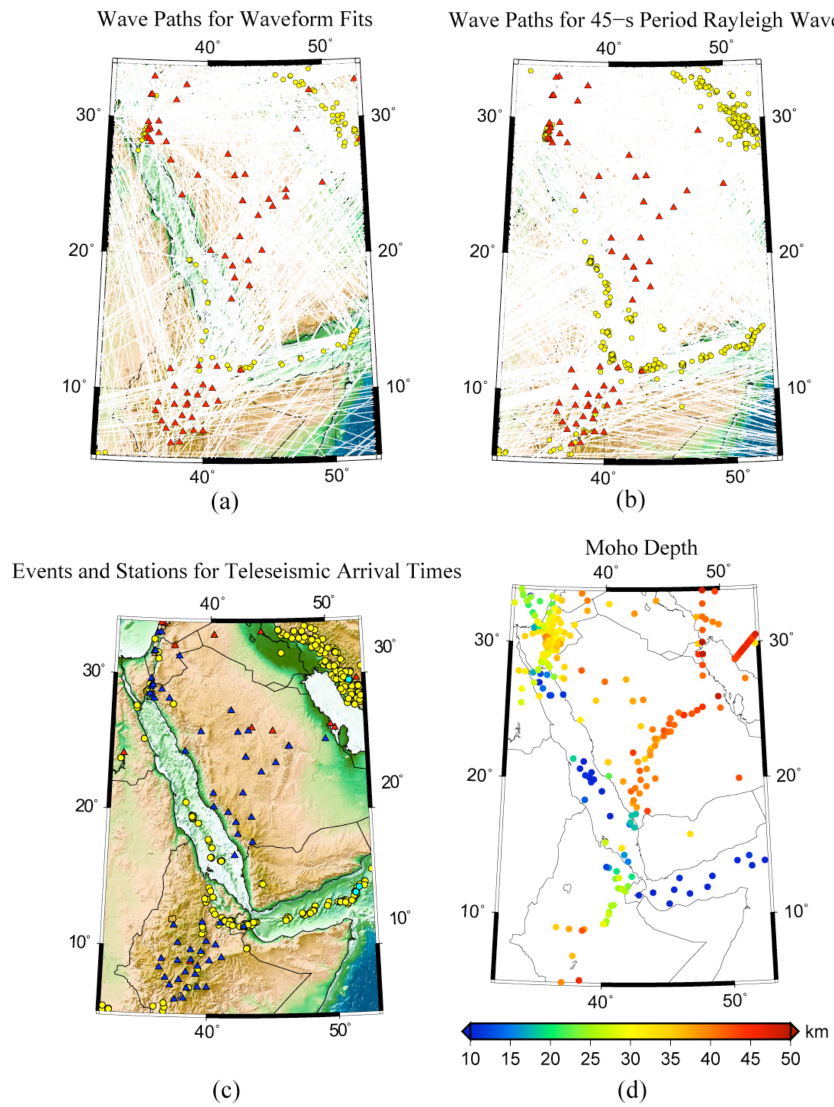

Fig. S1. Great-circle wave paths for (a) waveform fits and (b) 45-period Rayleigh waves. Stations and events are indicated in red triangles and yellow circles, respectively. (c) Location of events and stations for teleseismic arrival times. Stations and events from ISC database and multi-channel cross-correlation technique are indicated by red triangles, yellow circles, blue triangles and cyan circles, respectively. (d) Moho depth variations.

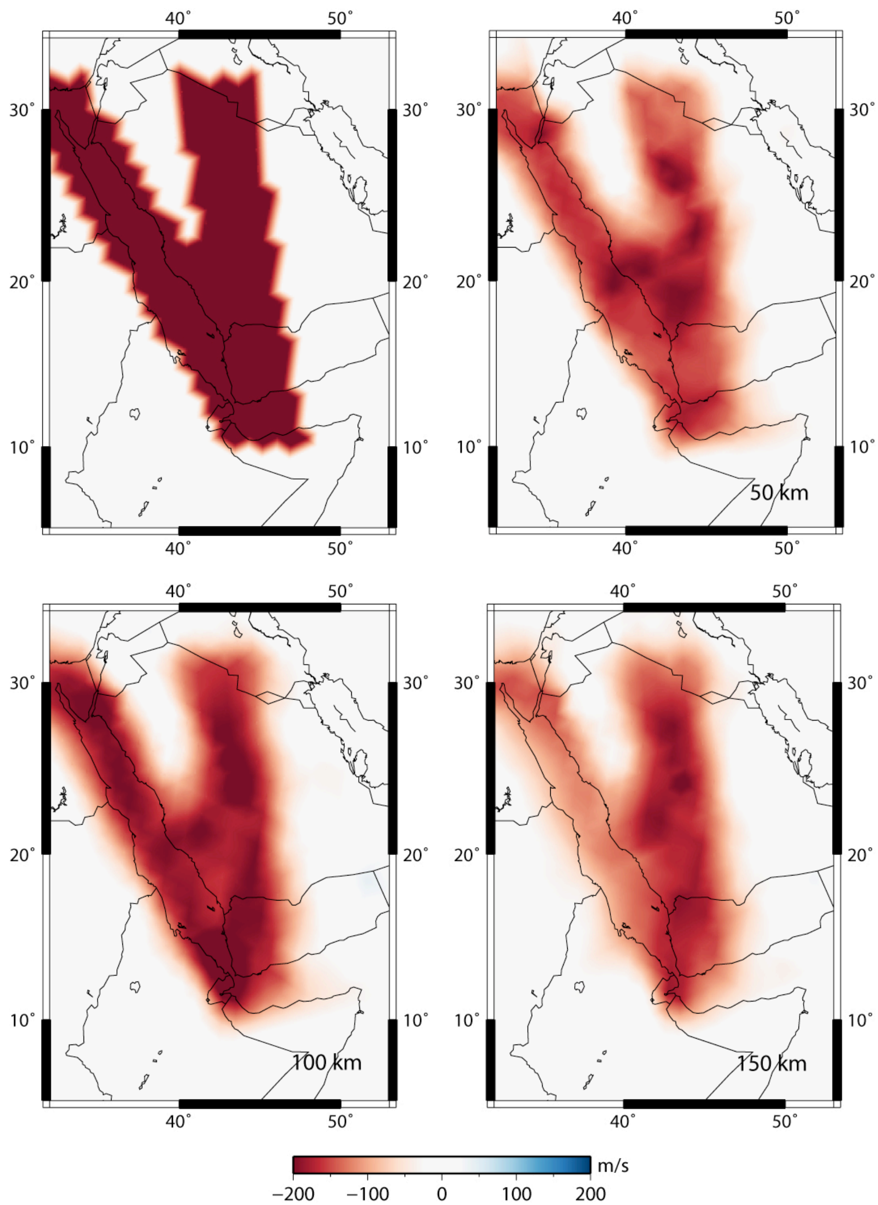

Fig. S2. Resolution test for a model including two separate low-velocity anomalies. The starting model is shown in the left-top panel, and inversion results are shown at 50, 100, and 150 km depths.

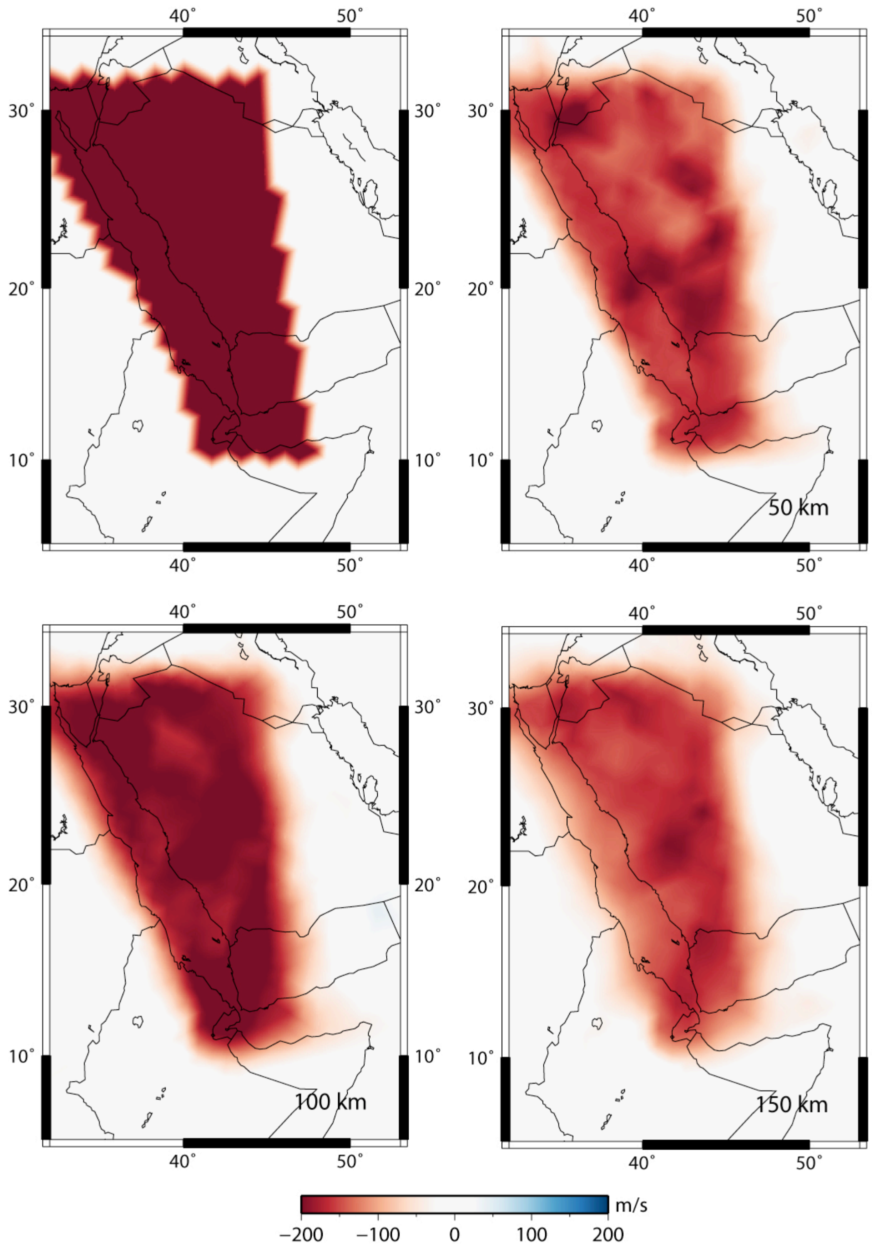

Fig. S3. Resolution test for a model including a broad low-velocity anomaly covering the Red Sea and western Arabia. The model is in the left-top panel, and inversion results are shown at 50, 100, and 150 km depths.

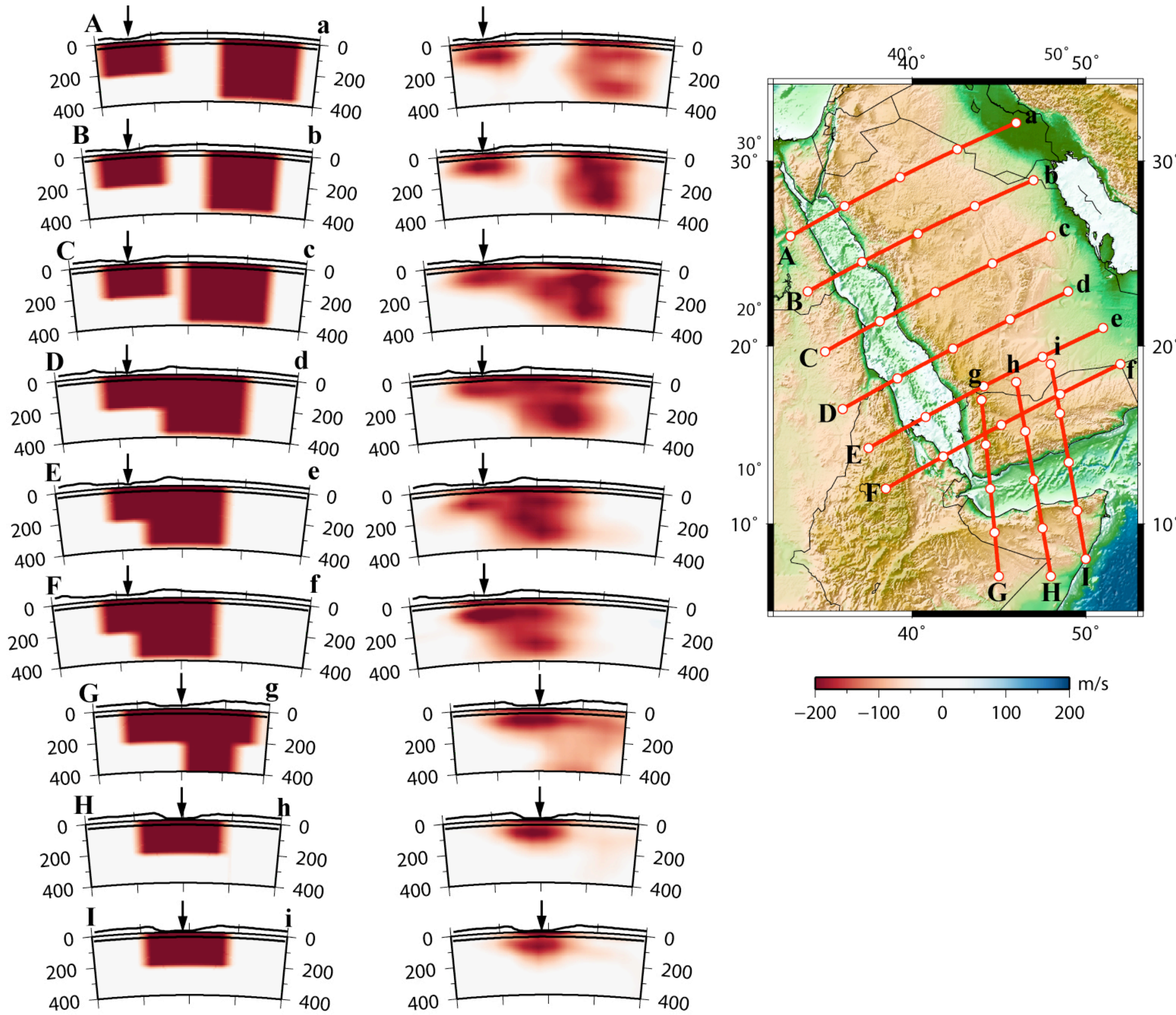

Fig. S4. Resolution test for cross sections along the Red Sea and the Gulf of Aden. The models are shown on the left, and the corresponding inversion results are given in the middle. Moho depth and surface topography are depicted in black solid lines. Topography is exaggerated 10 times. Black arrows indicate location of ridge on each cross section. Lines corresponding to the cross sections are shown on the map on the right. White circles on the great-circle paths correspond to ticks in the cross sections.

Supplementary References

Benoit, M. H., A. A. Nyblade, T. J. Owens and G. Stuart (2006), Mantle transition zone structure and upper mantle *S* velocity variations beneath Ethiopia: Evidence for a broad, deep-seated thermal anomaly, *Geochem., Geophys., Geosys., 7,* Q11013, doi:10.1029/2006GC001398.

Chang, S.-J., S. van der Lee, M. P. Flanagan, H. Bedle, F. Marone, E. M. Matzel, M. E. Pasyanos, A. J. Rodgers, B. Romanowicz, and C. Schmid (2010), Joint inversion for 3-dimensional S-velocity mantle structure along the Tethyan margin, *J. Geophys. Res.*, *115*, B08309, doi:10.1029/2009JB007204.

Engdahl, E. R., R. Van der Hilst, and R. Buland (1998), Global teleseismic earthquake relocation with improved travel times and procedures for depth determination, *Bull. Seismol. Soc. Amer., 88*, 722-743.

Nolet, G. (1990), Partitioned waveform inversion and 2-

dimensional structure under the network of autonomously recording seismographs, *J. Geophys. Res.*, *95*, 8499-8512.

Park, Y., A. A. Nyblade, A. J. Rodgers, and A. Al-Amri, A., (2007) Upper mantle structure beneath the Arabian Peninsula and northern Red Sea from teleseismic body wave tomography: Implication for the origin of Cenozoic uplift and volcanism in the Arabian Shield, Geochem., Geophys., Geosys., *8*, Q06021, doi:10.1029/2006GC001566.

Pasyanos, M. E. & A. A. Nyblade (2007), A top to bottom lithospheric study of Africa and Arabia, *Tectonophysics, 444*, 27-44.

Schmid, C., S. Van der Lee, and D. Giardini (2004), Delay times and shear wave splitting in the Mediterranean region: *Geophys. J. Intern., 159*, 275-290.

Van der Lee, S. and G. Nolet (1997), Upper mantle *S* velocity structure of North America, *J. Geophys. Res. 102*, 22,815-

22,838.

VanDecar, J. C. & R. S. Crosson (1990), Determination of teleseismic relative phase arrival times using multi-channel cross-correlation and least-squares, *Bull. Seisol. Soc. Amer., 80,* 150-169.